Density Functional Theory Molecular Cluster Study of Copper Interaction with Nitric Oxide Dimer in Cu–ZSM-5 Catalysts

ARTICLE *in* THE JOURNAL OF PHYSICAL CHEMISTRY C · JANUARY 2007

Impact Factor: 4.77 · DOI: 10.1021/jp0650634

Density Functional Theory Molecular Cluster Study of Copper Interaction with Nitric Oxide Dimer in Cu−ZSM-5 Catalysts

Ivan I. Zakharov,[†,‡] Zinfer R. Ismagilov,*[,†] Sergey Ph. Ruzankin,[†] Vladimir F. Anufrienko,[†] Svetlana A. Yashnik,[†] and Olga I. Zakharova[‡]

Boreskov Institute of Catalysis, Novosibirsk 630090, Russia and Severodonetsk Technological Institute of Volodymyr Dal East Ukrainian National University, Severodonetsk 93400, Ukraine

Received: August 7, 2006; In Final Form: December 5, 2006

The various quantum chemical models of catalytic active site in Cu−ZSM-5 zeolites are analyzed. The density functional theory (DFT) is used to calculate the electronic structure of molecular cluster $(HO)_3Al-O-Cu-O-Cu$ modeling the catalytic active site in Cu−ZSM-5 zeolites and study the interaction and decomposition of NO. It is assumed that the rate-determining stage of the low-temperature selective catalytic reduction of NO is the formation of the π-radical $(N_2O_2)^-$ on electron donor sites of Cu−ZSM-5 catalysts. This is in good agreement with the high electron affinity of the molecular dimer ONNO ($E_a = -1.5$ eV) and is confirmed by the experimental data on the formation of surface anion π-radical $(N_2O_2)^-$ on electron donor sites of supported organo−zirconium surface complex. The DFT calculated electronic structure and excitation energy spectra for the model system $(HO)_3Al-O-Cu-O-Cu$ show that it is a satisfactory model for description of experimental UV−vis spectra of Cu−ZSM-5, containing (−O−Cu−O−Cu−) chain structures in the zeolite channels. The calculated reaction energy profile of ONNO adsorption and decomposition on the model catalytic active site shows the possibility of the low-temperature decomposition of dimer $(NO)_2$ with low activation energy and the important role of copper oxide chains (−O−Cu−O−Cu−) in the channels of Cu−ZSM-5 zeolite during selective reduction of NO.

I. Introduction

After discovery of direct NO decomposition[1] and selective catalytic reduction (SCR) of NO by hydrocarbons[2,3] over copper-exchanged H-ZSM-5 zeolite (Cu−ZSM-5) zeolites, the interest in catalytic active sites of Cu−ZSM-5 and in activated forms of adsorbed NO grew considerably. Stabilization of isolated Cu^{2+} and Cu^+ ions,[4−8] as well as oxide CuO- and Cu_2O-like clusters,[9,10] ($[Cu-O-Cu]^{2+}$)[1,11−17] and (bis-[Cu-μ-$(O)_2$-Cu]$^{2+}$)[18−21] dimers, and (−Cu−O−Cu−O−) chain structures[22−25] in Cu−ZSM-5 has been observed by spectroscopic methods. These copper states each have been suggested to act as catalytic active sites in NO decomposition and SCR by hydrocarbons.

Earlier selective catalytic reduction of NO was believed to be due to its activation in the form of dimer $(NO)_2$.[11,13,26,27] The possibility of dimer $(NO)_2$ stabilization on the simplest active sites of Cu−ZSM-5 simulated as Cu^+ cations and its aquacomplexes was shown by quantum chemical analysis using density functional theory (DFT).[28]

We have observed isolated Cu^{2+} ions in zeolite cation-exchange positions, copper oxide chain structures in the zeolite channels, and square−plain oxide clusters by electron spin resonance (ESR) and diffuse reflectance spectroscopy.[22−25] The most interesting among the above states of copper ions are chain structures $Cu^{2+}-O^{2-}-Cu^{2+}-O^{2-}-$ because of the easiness of copper reduction and reoxidation in them as well the ability to stabilize bonded states of copper ions with mixed valence $Cu^{2+}\cdots Cu^+$.

The formation of copper oxide chain structures (−O−Cu−O−Cu−) in the channels of Cu−ZSM-5 zeolites, which is accompanied by the appearance of specific ligand−metal charge-transfer bands (CTB L → M) in the region 18 000−23 000 cm^{-1} of diffuse reflectance UV−vis spectra, has been shown in a series of our recent papers.[22−25] The investigation of the electronic structure of such groups and their preliminary quantum chemical analysis[22] showed that self-reduction {Cu(II)O(II) ⇔ Cu(I)O(I)} is possible for them. It results in the appearance of specific O^- ESR spectra[22,25] and specific intervalence charge transfer (IVT) bands Cu(II)/Cu(I) ⇔ Cu(I)/Cu(II) observed in region 15000−17000 cm^{-1} of diffuse reflectance UV−vis spectra.[23,25]

It is noted that a single instance of stabilization linear structures of transition metals ions is known. Stabilization of Fe cations as linear bi- and polynuclear iron oxo−hydroxo-complexes in zeolite channels is discussed with using data of Mossbauer spectroscopy.[29] Stabilization of linear-type clusters with average composition close to Cu_2O in zeolite channels ZSM-48 and ZSM-5 was proposed on base of EXAFS and XANES data.[30,31] EXAFS data showed that copper oxide in zeolites ZSM-48 and ZSM-5 possessed a Cu−O bond distance of 1.95 Å with coordination number of 1−2.[31] Because ZSM-48 and ZSM-5 possessed a channel opening of 5−6 Å, the possible sizes of the linear-type copper oxides in these confined pores were 2.93−2.95A.[31]

The observation of the IVT bands in UV−vis spectra of Cu−ZSM-5 definitely indicates that the Cu(I)/Cu(II) recharging potential is low for copper oxide chain structures in which stabilization of the "pair" copper state Cu(II)−e^-−Cu(II) is possible. Together with high electron affinity of the molecular dimer ONNO ($E_a = -1.3 \div -1.7$ eV),[32] this may result in the

* Corresponding author. E-mail: zri@catalysis.ru.
† Boreskov Institute of Catalysis.
‡ Severodonetsk Technological Institute of Volodymyr Dal East Ukrainian National University.

10.1021/jp0650634 CCC: $37.00
Published on Web 01/26/2007

TABLE 1: DFT Calculated Data of the Geometric and Electronic Structures for the $(NO)_2$ Dimer, Its π-Anion $(ONNO)^-$, and the $(HO)_3Al-O-Cu-O-Cu$ Complex as a Model of the Catalytic Active Site (CAS)[a]

	B3LYP/LANL2-DZ Calculations[b]		
molecular system (symmetry, state)	calculated geometry (Å)	electronic parameters	DFT/B3LYP energy (E)
cis-ONNO C_{2V}, ($^1A_1$)	r(N−N) = 1.99 (2.24) r(N−O) =1.16 (1.17) ∠NNO = 99.9° (90.9)	q(N) = +0.12 (+0.07) q(O) = −0.12 (−0.07)	E_{total} = −259.76844 au (−259.49330)
cis-$(ONNO)^-$ C_{2V}, ($^2B_1$)	r(N−N) = 1.40 (1.46) r(N−O) = 1.26 (1.23) ∠NNO = 115.8° (114.6)	q(N) = −0.05 (−0.31) q(O) = −0.45 (−0.19) ρ_s(N) = 0.12 (−0.01) ρ_s(O) = 0.38 (+0.51)	E_{total} = −259.81542 au (−259.55039) E = −1.3 eV (E = −1.55 eV)
complex $(HO)_3Al-O-Cu-O-Cu$ (Figure 1a) C_S, ($^3A''$)	r(Cu1−O1) = 1.80 r(Cu2−O1) = 1.76 r(Cu2−O2) = 1.76 r(Al-O2) = 1.87 r(Al−O) = 1.72 r(O−H) = 0.96 ∠Cu1O1Cu2 = 145.1° ∠O1Cu2O2 = 179.6° ∠AlO2Cu2 = 174.0°	Cu1($d^{9.84}s^{0.44}p^{0.16}$) Cu2($d^{9.52}s^{0.54}p^{0.24}$) q(Cu1) = +0.56 q(O1) = −0.67 q(Cu2) = +0.70 q(O2) = −0.61 ρ_s(Cu1) = 0.02 e ρ_s(O1) = 0.57 e ρ_s(Cu2) = 0.33 e ρ_s(O2) = 0.91 e q(AlO_3H_3) = +0.02 ρ_s(AlO_3H_3) = +0.17	E_{total} = −772.35564 au

[a] Checkpoint files contained wavefunction (molecular orbitals as linear combinations of atomic orbitals (MOLCAO)) and optimized geometry are available from NQMLab wavefunction dataebase.[41] [b] cis-ONNO dimer and anion π-radical $(ONNO)^-$ values calculated by CBS extrapolation are shown in parentheses.[46]

formation of surface anion π-radical $(ONNO)^-$ in such systems that is similar to the organo−zirconium surface complex with $(N_2O_2)^-$ observed by ESR.[33]

On the other hand, the formation of a strong bond between nitrogen atoms in such radical (N−N = 1.4 Å)[32] clearly indicates that decomposition of the intermediate form $-(N_2O_2)^-$ to a N_2O molecule and $-(O)^-$ is the preferred decomposition pathway. Indeed, the ONNO dimer adsorbed on the metal surface Ag-(111) shows a surprising low-temperature reactivity producing directly N_2O adsorbed molecules with a low activation energy of 2.0 kcal/mol: $(ONNO)_{ad} \Rightarrow N_2O_{ad} + O_{ad}$.[34,35] The dimer $(NO)_2$ has been clearly identified on the metal surface Cu(111).[36]

Thus, on the basis of the above data, it is natural to suppose that the rate-determining step of the low-temperature selective catalytic reduction of NO is the formation of the π-radical $(N_2O_2)^-$ on electron donor sites of Cu−ZSM-5 catalysts. One of possible electron donor sites in Cu−ZSM-5 is the copper oxide chain structure.

In the present study, we used DFT to calculate the electronic structure of molecular cluster $(HO)_3Al-O-Cu-O-Cu$ modeling a fragment of the copper oxide chain structure in Cu−ZSM-5 zeolites, comparison of their theoretical and experimental electronic spectra, and study the ONNO interaction and decomposition on this catalytic active site.

II. Quantum Chemical Model And Calculation Details

We analyzed various models to represent the structure of catalytic active site (CAS) in Cu−ZSM-5 zeolites. Detection of a Cu^+ site adjacent to one Al framework atom (Al−O−Cu) using a CO probe was recently reported.[37] The stronger π-electron donation due to such Cu site[37] is of more direct interest to us. Taking into account this fact and assuming stabilization of chain structures (−O−Cu−O−Cu−) in the zeolite channels,[22−25] we used the electronic structure of molecular cluster $(HO)_3Al-O-Cu-O-Cu$ modeling the catalytic active site in Cu−ZSM-5 zeolites and study the interaction of ONNO with this site. The molecular cluster $(HO)_3Al-O-Cu-O-Cu$ has a great number of possible electronic states because of the intermixing of oxygen p-orbitals and copper d-orbitals.[22−25] We found that the lowest energy state of this cluster corresponds to the S = 1 with spin populations on the oxygen atoms $[(HO)_3Al-O(\uparrow)-Cu-O(\uparrow)-Cu]$. This agrees well with the observation of the ESR spectra of O^- ion radicals for Cu−ZSM-5 zeolites.[22,24]

All calculations, geometry optimizations, and search of a transition state (TS) were performed with the Gaussian-98 package[38] at the DFT level using the hybrid exchange-correlation functional B3LYP.[39,40] The following basis set partition scheme was employed:

(a) The LANL2 effective core potential[41] with its valence shell basis set double-ζ (DZ) provided by the Gaussian-98 package was used for Cu and Al atoms. All atoms belonging to the $(HO)_3Al-O-Cu-O-Cu$ molecular cluster were described using the DZ basis set (B3LYP/LANL2-DZ calculations).

(b) The dimer $(NO)_2$ was described using the 6-31G* basis set.

The charge and spin density distributions on the atoms were calculated using the Mulliken population analysis. Open shells were calculated using unrestricted density functional calculations (uB3LYP/LANL2-DZ).

To allow one an exact reproduction of obtained DFT solutions for describing adsorbed species, Gaussian checkpoint files have been stored in NQMLab wavefunction database.[42]

Electronic Structure of Dimer $(NO)_2$ and $(HO)_3Al-O-Cu-O-Cu$ Cluster. Spontaneous NO dimerization has been observed in the gas phase at low temperature.[43−46] The results of the quantum chemical (B3LYP/6-31G*) calculation of the nitric oxide dimer, ONNO, are reported in Table 1. In accordance with the experimental data,[43−46] cis-ONNO structure with C_{2V} symmetry in $^1A_1$ singlet state has been found to be the most stable form of the nitric oxide dimer. The electronic structure of cis-ONNO dimer with 22 valence electrons may be presented in the following way (Scheme 1a):

(i) Six σ-electrons participate in the formation of three σ-bonds O−N, N−N, N−O.

(ii) Four π-electrons form two double bonds O−N and N−O.

(iii) Twelve electrons are localized in 6 lone pairs.

SCHEME 1: Schematic Representation of the Electron Structure of cis-ONNO Dimer (a) and Its Dianion $(ONNO)^{2-}$ (b); σ and π-bonds Are Shown as Lines, Lone Pairs as Lobes, and π-orbitals as Circles

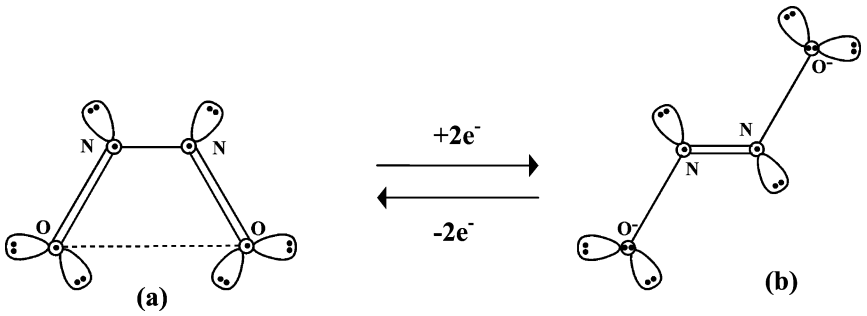

SCHEME 2: Molecular Structure of Occupied ($1b_1$ H $1a_2$) and Lowest Unoccupied ($2b_1$) π-orbitals of cis-ONNO Dimer. Spatial π-interaction of Two Oxygen Atoms Implements π- Conjugation of the Bonds and Stabilizes the cis Form of ONNO Dimer

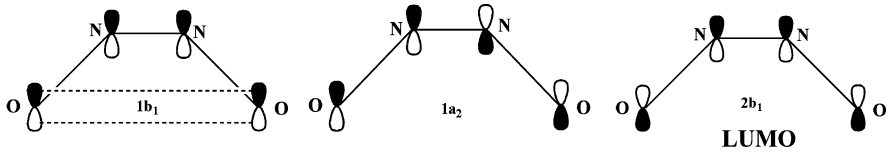

We believe that coupling of two π-bonds O−N and N−O by spatial π-interaction of two oxygen atoms stabilizes the cis form of the ONNO dimer. This conclusion is supported by the low valence angle ∠NNO = 97.2° and calculations of $(ONNO)^{2-}$ dianion[32] leading to the stabilization of the trans structure of the dimer when oxygen π-orbitals are filled with the formation of π-lone pairs (Scheme 1b).

Another feature of the electronic structure of the molecular cis-ONNO dimer ($^1A_1$) is the presence of a low lying unoccupied molecular orbital (LUMO), which is a binding π-orbital for nitrogen atoms (Scheme 2).

Therefore, in contrast to the molecular weakly bonded cis dimer with the equilibrium N−N distance ∼2 Å, according to the results of Snis and Panas,[32] anion π-radical $(ONNO)^-$ must be characterized by a strong bond between nitrogen atoms (N−N ≈ 1.4 Å). Of great importance for stabilization of anion π-radical $(ONNO)^-$ over electron donor surface sites is the electron affinity of the ONNO dimer. We carried out a quantitative estimation of this value using complete basis set (CBS) extrapolation at the forth-order Moller−Plesset level of theory.[47] For estimation of the electron affinity, the calculation of molecular cis-ONNO dimer ($^1A_1$ term) and its anion $(ONNO)^-$ ($^2B_1$ term) was performed by CBS method and gave the following results: R_{N-N} = 2.241 (1.460) Å, R_{N-O} = 1.174 (1.232) Å, ∠NNO = 90.85° (114.6°), E(CBS) = −259.493302 (−259.550394) au. The results obtained for the π-anion are reported above in the parentheses. These results of the calculation of cis-ONNO dimer ($^1A_1$ term) geometry adequately reproduce the experimental data[44] (R_{N-N} = 2.263 Å, R_{N-O} = 1.152 Å, ∠NNO = 97.2°. The calculated high electron affinity of the molecular dimer ONNO (E_a = −1.5 eV) is in good agreement with the results of calculations at the B3LYP/6-311+G* level ($E_a \approx -1.3 \div -1.7$ eV).[32] The B3LYP/6-31G* calculations in this work give E_a = −1.3 eV and confirm the experimental data on the formation of surface anion π-radical $(N_2O_2)^-$ on electron donor sites of supported organo−zirconium surface complex.[33]

We used the molecular cluster $(HO)_3$Al−O2−Cu2−O1−Cu1 (Figure 1a) to model the CAS in Cu−ZSM-5 zeolites and to study its interaction with ONNO. Table 1 presents the optimized geometry and calculated atomic population of Cu 3d-orbitals as well as charge (q) and spin density distribution (ρ_s) on the atoms in CAS. We found that the lowest energy state of the model cluster corresponds to the spin S = 1 with calculated

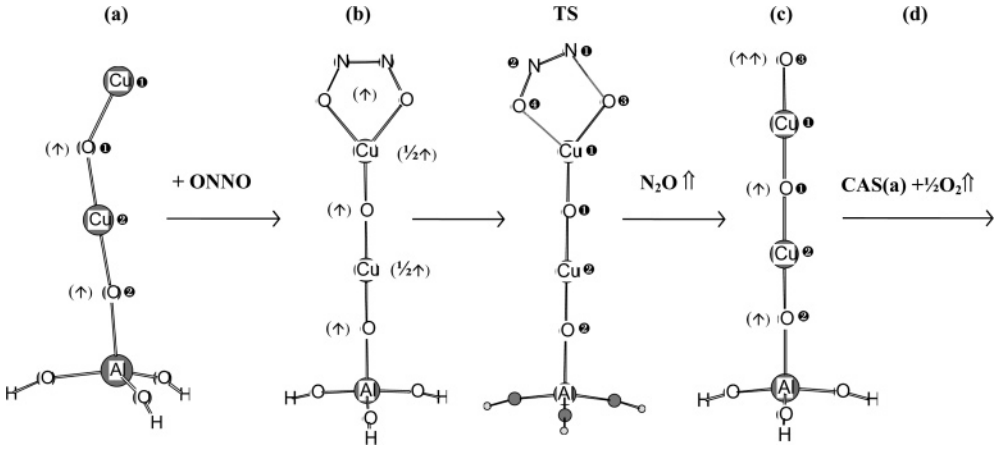

Figure 1. The DFT/LANL2-DZ calculated molecular structures formed after the interaction of complex $(HO)_3$Al−O−Cu−O−Cu (a) as a model of the catalytic active site with ONNO at addition and decomposition reaction steps (a + ONNO ⇒ b ⇒ TS ⇒ $N_2O\uparrow$ + c ⇒ d). The optimized molecular structures have different spin populations on atoms (shown in brackets). The calculated electronic structures and interatomic distances are shown in Table 1.

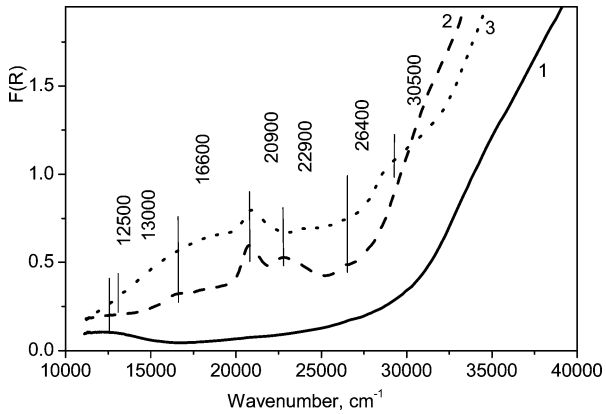

Figure 2. UV−vis spectra of 0.65% Cu−ZSM-5-30-38 prepared by ion exchange in aqueous solution of copper nitrate at 80 °C without washing and by following drying in air and calcinations at 500 °C. (1), initial sample; (2), after vacuum treatment at 150 °C for 1 h; (3), after vacuum treatment at 300 °C for 1 h.

spin density on the oxygen atoms: $\rho_s(O1) = 0.6$ e and $\rho_s(O2) = 0.9$ e. We believe that these results are consistent with the observation of the ESR spectrum of O^- ion radicals for Cu−ZSM-5 zeolites.[22,25] The calculated geometry of model CAS is almost linear: ∠O1Cu2O2 = 179.6° and ∠AlO2Cu2 = 174.0°. Only ∠Cu1O1Cu2 = 145.1° angle is smaller than 180°. In our opinion, this fact reflects the existence of interelectron interaction Cu1−Cu2. It may say that the electronic state Cu1-($d^{9.84}s^{0.44}p^{0.16}$) corresponds to the formal oxidation state Cu(I) with d^{10} electron configuration and with spin density $\rho_s(Cu1) \approx 0$e, whereas Cu2($d^{9.52}s^{0.54}p^{0.24}$) is characterized by spin density $\rho_s(Cu2) = 0.33$ e. Both Cu d-populations and atomic charges q(Cu1) = +0.56 and q(Cu2) = +0.70 indicate an oxidation state of Cu1 and Cu2 closer to Cu(I) than to Cu(II). Nevertheless, the calculations (Table 1) clearly indicate the tendency of the CAS electron structure to the state with different oxidation states Cu1(I) and Cu2(II).

Experimental and Theoretical Electronic Spectra and Aquation Effect. Figure 2 shows the experimental UV−vis spectra of Cu−ZSM-5 prepared by ion exchange of H−ZSM-5 with aqueous solution of copper nitrate, by following drying in air and calcination at 500 °C for 2 h, the initial sample (curve 1), and after vacuum heat treatments of the sample at 150 °C (curve 2) and at 300 °C (curve 3).[24,25] Adsorption bands in region 12 000−13 000 cm^{-1}, 15 000−17 000 cm^{-1}, 18 000−23 000 cm^{-1}, and 30 000−32 000 cm^{-1} have been observed in experimental UV−vis spectra of Cu−ZSM-5. It is known that the band 12 000−13 000 cm^{-1} is determined by d−d transition of isolated Cu^{2+} ions stabilized in octahedral crystal fields with small tetragonal distortion, which are created by oxide ligands.[23−25] This conclusion agree with ESR data for isolated Cu^{2+} ions.[4,6,22,25] The intensive band in 30 000−32 000 cm^{-1} is identified as CTB L → M corresponding to square−plain oxide clusters.[24,25] The origin of two bands 15 000−17 000 cm^{-1} and 18 000−23 000 cm^{-1} is not known and we assume that these bands are arising from copper oxide chain structures in zeolite channels. The first band can be ascribed to an intervalence transitions Cu(II)Cu(I) ↔ Cu(I)Cu(II). The second band can be considered as a charge-transfer ligand−metal.

The excitation energy spectra were calculated for the $(HO)_3Al$−O2−Cu2−O1−Cu1 cluster (Figure 1a) modeling of the copper oxide chain structure. This model containing two transition metals linked by a bridging oxygen atom is a good molecular system for investigation of the intervalence charge-transfer phenomena[48] because it allows the transfer of an electron from one metal to the other. The spectra were calculated in the frames of DFT approach taking into account the time-dependent perturbations[49] and using the same basis LANL2-DZ and optimized geometry of this cluster. This more general DFT method realized by Runge and Gross[50] was subsequently called time dependent density functional theory (TDDFT). First, the TDDFT method was used for calculation of the excitation energies, dynamic polarization, hyperpolarization, and Van der Waals dispersion coefficients for a collection of relatively simple molecules.[51−55] For some reason, few results were obtained for systems containing transition metals.[55−58] In this work, we applied the TDDFT method for calculations of the electronic spectra of a model complex containing transition metals in different spin states. Visualization of the orbitals and the spectra was performed by means of ChemCraft computer program.[59]

The excited states and corresponding oscillator strengths were calculated for 30 energy transitions in the range of 3000−25 000 cm^{-1}. For comparison with the experimental spectra, the calculated discrete spectrum was broadened by applying the Lorentz distribution with a half-width of 1000 cm^{-1}. The calculated spectra include the three most intense peaks at ∼12 000, 14 000, and 17 500 cm^{-1} and three low-intensity peaks at ∼8600, 16 000, and 20 400 cm^{-1} (Figure 3). Each excitation in the region of 15 000−23 000 cm^{-1} is composed of d−d, intervalence transitions, and charge transfer at a different ratio and hence includes more than one molecular (delocalized) orbital

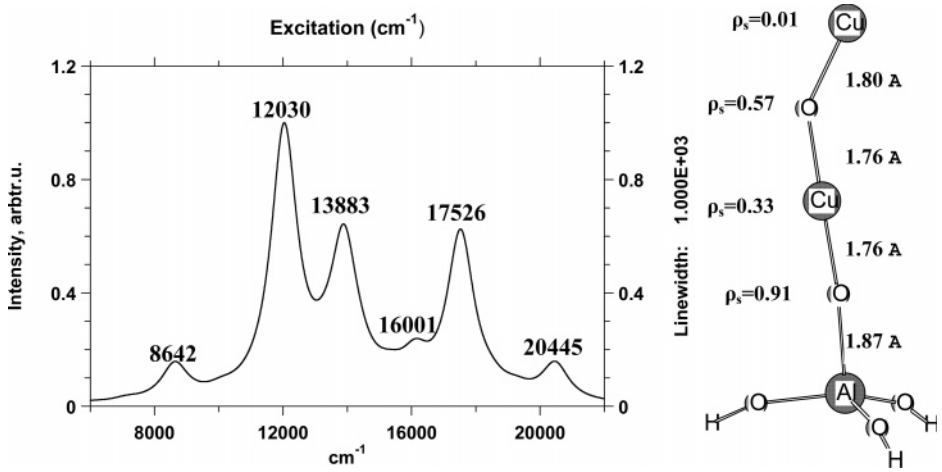

Figure 3. Calculated electron transition spectra of the $(HO)_3Al$−O−Cu−O−Cu complex with optimized geometry (Table 1). The spectra were broadened by applying the Lorentz distribution with 1000 cm^{-1} half-width to discrete transitions in region of d−d and intervalence bands.

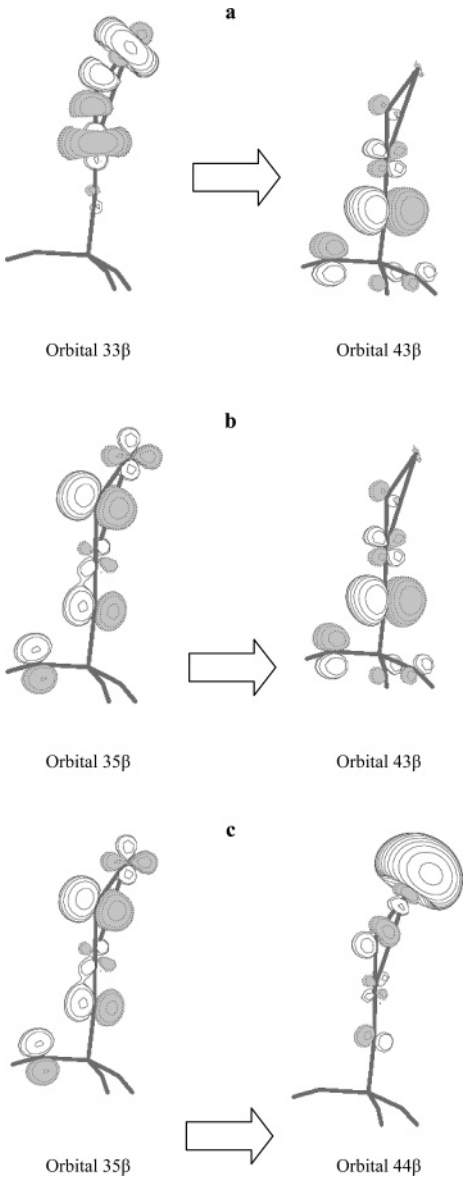

Figure 4. Examples of pairs of initial and final orbitals for $(HO)_3Al-O-Cu-O-Cu$ complex participating in intervalence and charge-transfer transitions. Each transition may involve several (delocalized) orbital pairs: (a,b), intervalence transitions from Cu1−O1 bond to Cu2−O2 bond; (c), charge-transfer transition from Cu2−O2 bond to Cu1−O1 bond. Contributions of each orbital pair to main peaks of calculated spectra are given in Table 2.

pair. For simplicity, the molecular orbitals localized mainly on $Al(OH)_3$ group and simulating the substrate were excluded from the analysis of the spectra. The principal molecular orbital pairs involved in the intervalence transitions in region of 15 000−17 000 cm^{-1} and the charge-transfer transitions in region of 18 000−23 000 cm^{-1} are shown in Figure 4a,b and Figure 4c, respectively. The contributions of each orbital pair to main peaks of calculated spectra are given in Table 2. According to Figure 4 and Table 2, all six absorption bands contain the transitions with participation of bridging oxygen atoms O1 and O2. This means that because of strong intermixing of oxygen p-orbitals with copper d-orbitals,[22,23] the intervalence transfer of the electron density goes mainly from Cu1−O1 bond to Cu2−O2 bond. The first five calculated absorption bands can be assigned to Cu(I) → Cu(II) and Cu(II) → Cu(I) intervalence transitions. The latter band at 20 445 cm^{-1} can be mainly assigned to band of charge-transfer ligand−metal O1−Cu1.

TABLE 2: Contributions of the Orbital Pair of Intervalence and Charge-Transfer Transitions to Main Peaks of Calculated Spectra

peak, cm^{-1}	initial orbitals	final orbitals	contribution to transition
8642	35β	43β	0.26 (IVT)
12 030	35β	43β	0.43 (IVT)
13 883	35β	43β	0.30 (IVT)
	33β	43β	0.22 (IVT)
16 001	35β	43β	0.37 (IVT)
	33β	43β	0.36 (IVT)
17 526	33β	43β	0.41 (IVT)
20 445	35β	44β	0.41 (CTB)
	35β	43β	0.34 (IVT)

So, we believe that the $(HO)_3Al-O2-Cu2-O1-Cu1$ complex (Figure 1a) is a satisfactory model for the description of experimental UV−vis spectra of Cu−ZSM-5 zeolites in range of 15 000−23 000 cm^{-1} and may be used for further calculations.

In the discussed CAS model, the three OH fragments bonded with the Al atom that simulate the effect of the zeolite matrix were considered to be absolutely equivalent during the geometry optimization. To test the effect of this limitation on the obtained energetic and spectral characteristics of the model, additional calculations were performed for models in which this limitation was removed. Independent optimization of the OH groups in the $Al(OH)_3$ fragment led to the following effects:

(a) Slight deformation of the $Al(OH)_3$ fragment without change of the geometry of the (−O−Cu−O−Cu-) chain (Figure 5a) with a small energy decrease (by ∼0.2 kcal/mol).

(b) Small decrease of the spin density on the closest to aluminum oxygen atom of the chain from 0.91 to 0.88.

(c) Change in the shape of the calculated UV−vis spectra due to the effect of the support.

The latter results from a redistribution of the peak intensities, which is caused by the fact that the support simulated by the $Al(OH)_3$ fragment has certain contribution to each peak. Therefore, the change of the fragment geometry alters the positions and intensities of the peaks in the UV−vis spectrum.

The effect of hydration on the CAS physicochemical characteristics was studied by adding one or several water molecules to the coordination sphere of the copper atoms in the chain. LANL2DZ basis set was used for the water molecules. The results of the geometry optimization are presented in Figures 5, 6, and Table 3. The addition of one water molecule results in a considerable energy gain by 41 kcal/mol (Figure 5b). Meanwhile, the CAS geometry is practically unchanged. The spin density shifts slightly along the chain in the direction of the hydrated end. The charges on the chain atoms change in a more complex manner (Table 4). It is important to note that the UV−vis spectra do not change much. The absorption bands shift to higher energies by ∼1000−2000 cm^{-1}.

The introduction of several water molecules near the terminal copper atoms leads to strong coordination of one additional water molecule. The other water molecules do not bind with the terminal copper atom and are located at 2.68 Å distance from it (Figure 6A). The strong coordination of the second H_2O molecule leads to additional energy gain by 21 kcal/mol. The spin density at the hydrated copper atom grows significantly (by ∼0.2). In general, the spin density along the chain averages out (i.e., the spin properties of (Cu1−O1) and (Cu2−O2) groups become very similar). Undoubtedly, this change could be revealed in the UV−vis spectra, especially in the peaks related to intervalence transitions. Note that only two water molecules additionally bind with the second copper atom as well (Figure 6b). These results indicate that redistribution of the electron and

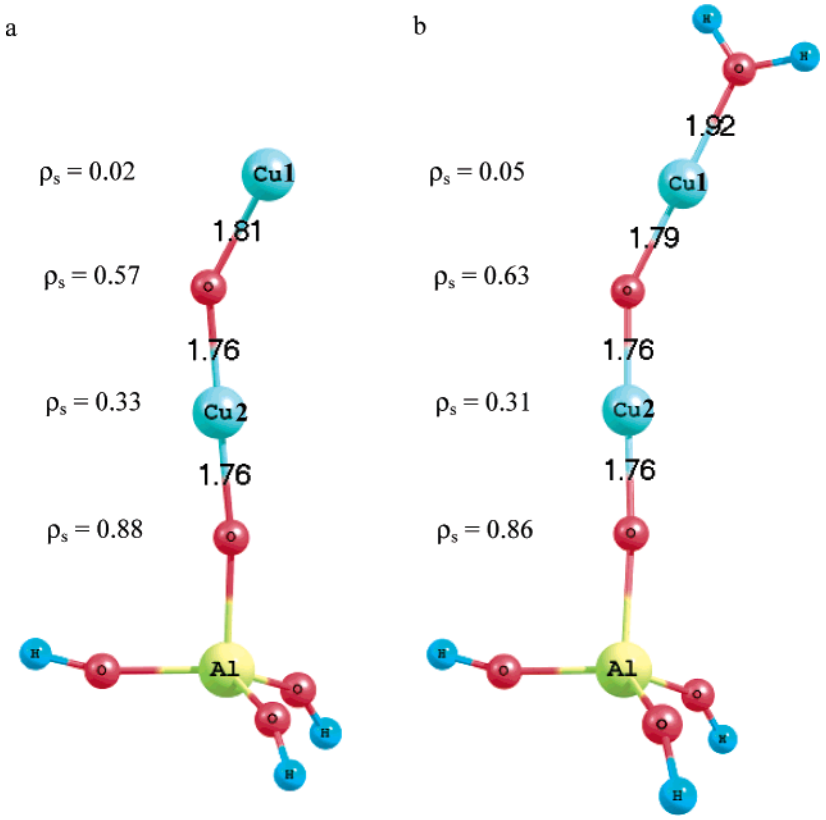

Figure 5. The change of the geometry and spin density ρ_s of CAS by hydration. (a) $(HO)_3Al-O-Cu-O-Cu-CAS$; (b) CAS + H_2O.

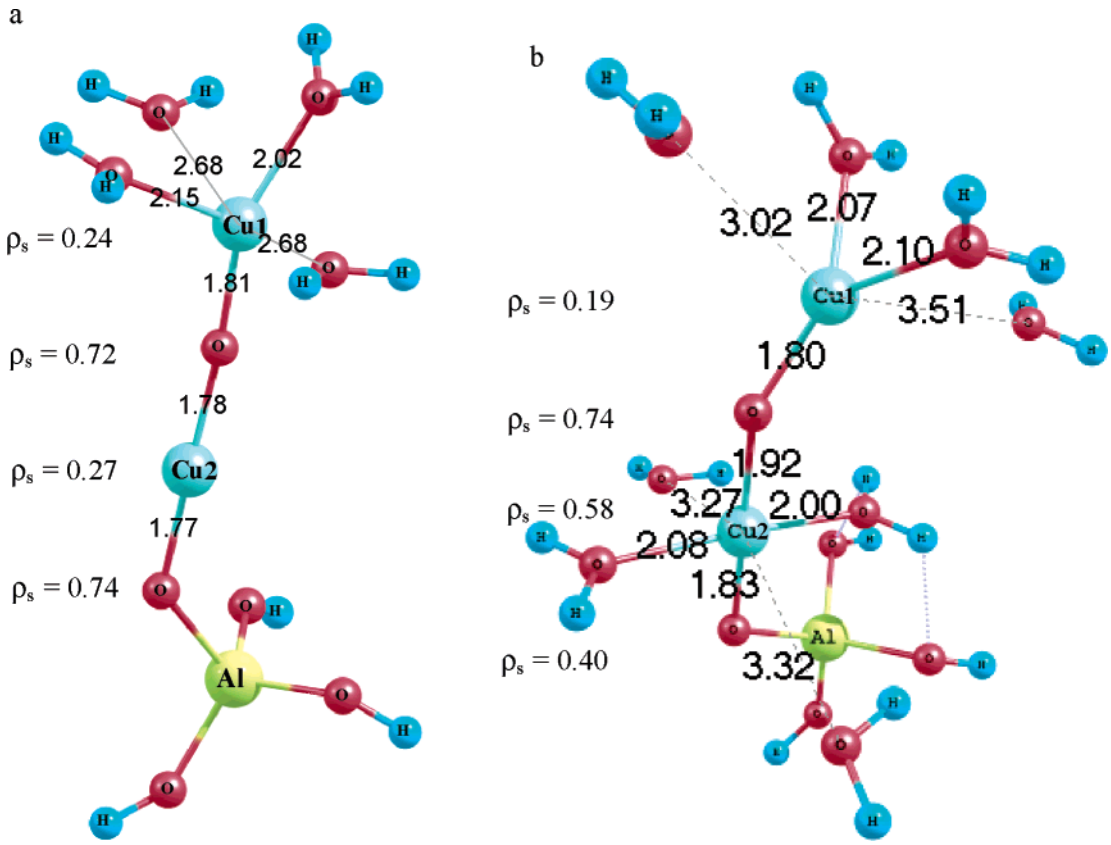

Figure 6. The geometry and spin density ρ_s of hydrated CAS: (a) CAS + 4 H_2O; (b) CAS + 8 H_2O.

spin densities corresponding to Cu(I) oxidation to Cu(II) takes place during hydration.

Figure 7 presents the UV−vis spectrum calculated for the hydrated model presented in Figure 6a. Only two intense peaks are observed at 14 300 and 19 300 cm^{-1} instead of the complex profile shown in Figure 3. Note that the low-energy peak consists of only one transition (14 260 cm^{-1}), whereas the latter one is composed of two transitions at 19 234 and 19 245 cm^{-1}

TABLE 3: Effect of Hydration

system	energy, au	ΔE, kcal/mol
$(HO)_3Al-O-Cu-O-Cu$ (CAS)	−772.35604	
H_2O	−76.41431	
CAS + H_2O	−848.77035	0
Hydrated (H_2O) CAS	−848.83506	−41
CAS + 4 H_2O	−1078.01330	0
Hydrated (4H_2O) CAS	−1078.11237	−62
CAS + 8 H_2O	−1383.67055	0
Hydrated (8H_2O) CAS	−1383.79742	−80

TABLE 4: Effect of Hydration on the Charges and Spin Density on the Atoms of the Chain

charge/spin density	CAS	CAS·H_2O	CAS·4H_2O	CAS·8H_2O
q(Cu1)	+0.57	+0.49	+0.57	+0.50
q(O1)	−0.66	−0.67	−0.66	−0.62
q(Cu2)	+0.70	+0.67	+0.59	+0.60
q(O2)	−0.63	−0.65	−0.68	−0.81
ρ_s(Cu1)	0.02	0.05	0.24	0.19
ρ_s(O1)	0.57	0.63	0.72	0.74
ρ_s(Cu2)	0.33	0.31	0.27	0.58
ρ_s(O2)	0.88	0.86	0.74	0.40

with approximately equal intensities. A more detailed analysis indicates that the transition in the region of 14 300 cm^{-1} consists mostly from three contributions of β-orbitals: $57\beta \rightarrow 63\beta$ (0.29), $59\beta \rightarrow 62\beta$ (0.24), and $60\beta \rightarrow 63\beta$ (0.87). Their contributions to overall excitation is shown in the parentheses. The first contribution is an intervalence transition (Cu1−O1) → (Cu2−O2), the second one is the reverse transition (Cu2−O2) → (Cu1−O1), and finally the last major contribution consists mainly of the electron density transfer from the support to the chain: $(O)_3 \rightarrow$ (O2−Cu2−O1) with a minor admixture of the (Cu1−O1) → (Cu2−O2) transfer. The two adjacent transitions contributing to the second peak in the 19 300 cm^{-1} region have a more complex origin. They mostly consist of charge-transfer transitions $(O)_3 \rightarrow$ (O2−Cu2−O1) (0.64 ÷ 0.70) and (Cu2) → (O2−O1) (0.63) with participation of intervalence transitions (Cu1−O1) → (Cu2−O2) (0.27 ÷ 0.42).

Further hydration results in the shift and splitting of the absorption bands (Figure 8). Peaks in region 22 400 cm^{-1} and 23 800 cm^{-1} consist of the charge transfer of electronic density from metal to ligands (oxygen of chain and water molecules). As hydration proved to be energetically favorable (Table 5), one can expect that it will result in a significant change in the coordination of copper atoms to the point of the $[O-Cu(H_2O)_2-O-Cu(H_2O)_2]$ type structure with weakening of the Cu−O bond in the chain and spin density transfer to the copper atoms reaching the value $\rho_s \sim 0.6$.

Thus, hydration is energetically favorable and results in a significant decrease in the total number of transitions in the energy range below 25 000 cm^{-1} and significant change of the spectrum profile that could be observed experimentally.

Electronic and Molecular Structure of a Complex Formed after Interaction of Model CAS with ONNO. DFT quantum chemical analysis of the $(NO)_2$ stabilization over the simplest model active sites of Cu−ZSM-5 in the form of Cu^0, Cu^+, and Cu^{2+} cations and their aquacomplexes[28] showed that N-down coordination with stabilization of Cu−dinitrosyl complexes is typical for Cu^+ and Cu^{2+} electron acceptor sites. At the same time, only O-down structures are stable with neutral Cu sites so that charge and orbital analyses are consistent with the description of the cluster $[(H_2O)_xCu(I)-(O_2N_2)^-]$.[28] This is in good agreement with the X-ray diffraction (XRD) data on the platinum complex $(Ph_3P)_2Pt(O_2N_2)$ that has a cis-hyponitrite ligand, which bonds to platinum through the oxygen atoms to

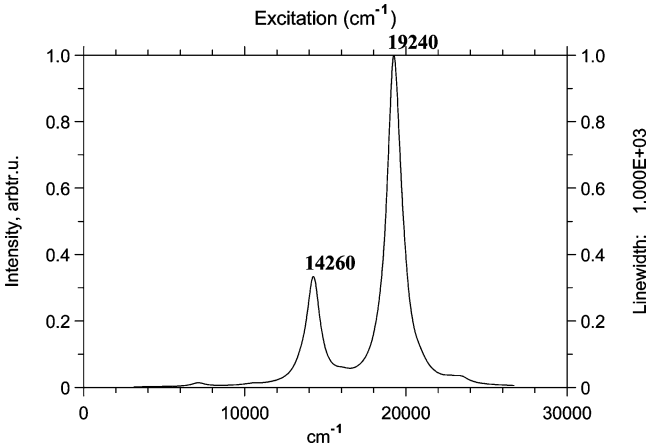

Figure 7. UV−vis spectrum of CAS hydrated by two strong coordinated H_2O molecules (Figure 6a, 2 H_2O + 2 H_2O).

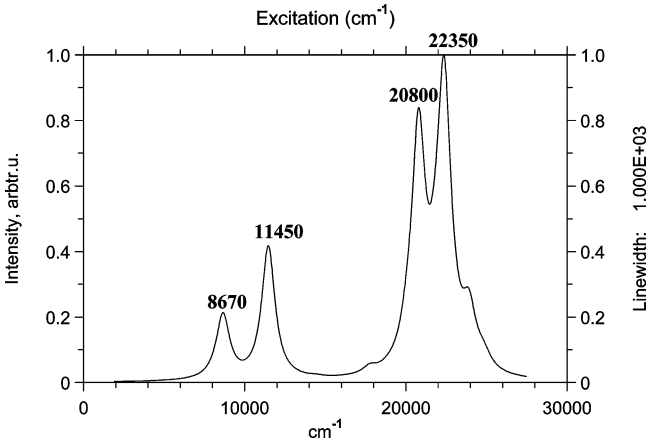

Figure 8. UV−vis spectrum of CAS hydrated by four strong coordinated H_2O molecules (Figure 6b, 4 H_2O + 4 H_2O).

give a bidentate hyponitrite structure with a relatively short N−N bond (1.2−1.3 Å).[60] Using these results and the B3LYP/LANL2-DZ method, we calculated the geometric and electronic structures of the CAS donor−acceptor interaction with the cis-ONNO dimer through the oxygen atoms (Figure 1b). We found that the lowest energy state of the CAS−hyponitrite complex corresponds to the S = 2 spin. Table 5 shows that the charge densities and spin populations of the CAS−hyponitrite complex are consistent with the description $[CAS^+-(O_2N_2)^-]$ and the optimized geometry has a relatively short N−N bond (1.34 Å). Such a structure may be associated with greater electron donation of CAS. Comparison of calculation results for isolated CAS (Table 1) and CAS−ONNO (Table 5) complexes indicates that the electron density donation to the dimer is mainly implemented through the decrease of the electron density on Cu1. Note that the electron state of Cu2 before and after interaction with ONNO is practically the same (see Table 1 and 5), whereas the electron density transfer from the $Al(OH)_3$ fragment to the ONNO dimer proved to be significant [$q(Al(OH)_3) = +0.18$; $\rho_S(Al(OH)_3) = +0.35$]. The calculated bond energy CAS−ONNO is $\Delta H = -29.4$ kcal/mol ($\Delta G_{298} = -14.9$ kcal/mol) (see Table 5). Although the Cu−hyponitrite complexes may not be stable enough to be observed experimentally in Cu−zeolite, they may play an important role in N−N bond forming processes. As the decomposition of the hyponitrite complex to N_2 and O_2 is symmetry forbidden,[28] we considered an ONNO decomposition mechanism based on single-step disproportionation of CAS−hyponitrite complex to free N_2O and adsorbed O (see Figure 1).

TABLE 5: DFT Calculated Data of the Geometric and Electronic Structures for the CAS−Hyponitrite Complex and the Transition State of ONNO Decomposition

	B3LYP/LANL2-DZ Calculations		
molecular system (symmetry, state)	calculated geometry (Å)	electronic parameters	DFT/B3LYP energy (E)
complex	r(Cu1−O1) = 1.79	Cu1($d^{9.49}s^{0.44}p^{0.30}$)	E_{total} = −1032.17089 au
$(HO)_3Al-O-Cu-O-Cu$ + ONNO	r(Cu2−O1) = 1.76	Cu2($d^{9.50}s^{0.52}p^{0.22}$)	
	r(Cu2−O2) = 1.76	q(Cu1) = +0.77	ΔE = −29.4 kcal/mol[a]
	r(Al−O2) = 1.86	q(O1) = −0.69	
	r(Al−O)=1.72	q(Cu2)= +0.76	
(Figure 1b)	r(O−H) = 0.96	q(O2) = −0.61	
C_1, (^{5}A)	∠Cu1O1Cu2 = 175.6°	ρ_s(Cu1) = 0.45 e	
	∠O1Cu2O2 = 178.3°	ρ_s(O1)= 0.71 e	
	∠AlO2Cu2 = 171.6°	ρ_s(Cu2) = 0.37 e	
		ρ_s(O2) = 0.93 e	
	r(Cu1−O) = 1.95		
	r(N−O) = 1.28	q(ONNO) = −0.41	
	r(N−N)=1.34	ρ_s(ONNO) = 1.19 e	
		q(AlO_3H_3) = +0.18	
		ρ_s(AlO_3H_3) = +0.35	
transition state	r(Cu1−O1) = 1.79	Cu1($d^{9.47}s^{0.43}p^{0.32}$)	E_{total} = −1032.12989 au
(Figure 1, TS)	r(Cu2−O1) = 1.76	Cu2($d^{9.49}s^{0.52}p^{0.23}$)	
C_1, (^{5}A)	r(Cu2−O2) = 1.76	q(Cu1) = +0.78	ΔE = −3.7 kcal/mol
	r(Al-O2)=1.86	q(O1) = −0.69	
	r(Al−O)=1.72	q(Cu2) = +0.76	
	r(O−H)=0.96	q(O2) = −0.61	
	∠Cu1O1Cu2 = 175.7°	ρ_s(Cu1) = 0.44 e	
	∠O1Cu2O2 = 179.7°	ρ_s(O1) = 0.70 e	
	∠AlO2Cu2 = 179.3°	ρ_s(Cu2) = 0.37 e	
		ρ_s(O2) = 0.93 e	
	r(Cu1−O3) = 1.86		
	r(Cu1−O4) = 2.01	q(ONNO) = −0.41	
	r(N1−O3) = 1.86	ρ_s(ONNO) = 1.21 e	
	r(N2−O4) = 1.27		
	r(N−N) = 1.18	q(AlO_3H_3) = +0.17	
	<NNO = 134.0°	ρ_s(AlO_3H_3) = +0.35	
	∠O3Cu1O4 = 87.3°		
	∠Cu1O3N1 = 105.0°		

[a] The binding energy is calculated in approximation: $\Delta E = E_{total}$ (CAS−ONNO complex) − E_{total} (CAS-complex) − E_{total} (ONNO) = −29.4 kcal/mol.

TABLE 6: DFT/B3LYP Calculated Data of the Geometric and Electronic Structures of the Decomposition Reaction Products (Figure 1)

	B3LYP/LANL2-DZ Calculations[a]		
molecular system (symmetry, state)	calculated geometry (Å)	electronic parameters	DFT/B3LYP energy (E)
complex	r(Cu1−O3) = 1.725	q(O3) = −0.33	E_{total}= −847.50816 au
$(HO)_3Al-O-Cu-O-Cu-O_{ad}$	r(Cu1−O1) = 1.77	Cu1($d^{9.54}s^{0.54}p^{0.24}$)	
	r(Cu2−O1) = 1.76	Cu2($d^{9.49}s^{0.51}p^{0.23}$)	
(Figure 1c)	r(Cu2−O2) = 1.75	q(Cu1) = +0.68	
C_S, (^{5}A')	r(Al−O2) = 1.86	q(O1) = −0.66	
	r(Al−O) = 1.72	q(Cu2) = +0.77	
	r(O−H) = 0.96	q(O2) = −0.60	
	∠Cu1O1Cu2 = 178.0°	ρ_s(O3) = 1.37 e	
	∠O1Cu2O2 = 178.2°	ρ_s(Cu1) = 0.34 e	
	∠AlO2Cu2 = 170.1°	ρ_s(O1) = 0.66 e	
		ρ_s(Cu2) = 0.38 e	
		ρ_s(O2) = 0.94 e	
		q(AlO_3H_3) = +0.17	
		ρ_s(AlO_3H_3) = +0.31	
NNO			
$C\infty$ - ($^1\Sigma g$)	r(N−N) = 1.13 (1.128)	q(N1) = +0.53	E_{total} = −184.65624 a.u.
	r(N−O) = 1.19 (1.184)	q(N2) = −0.10	
		q(O) = −0.43	
O−O			
$C\infty$, ($^3\Sigma g$)	r(O−O) = 1.21 (1.207)	q(O) = 0.0	E_{total} = −150.31660 a.u.

[a] For N_2O ($^1\Sigma g$) and O_2 ($^3\Sigma g$), experimental equilibrium distances are shown in parentheses.

Electronic and Molecular Structure of the Decomposition Reaction Transition Complex. We analyzed theoretically the possibility of the adsorbed ONNO disproportionation on a model site of Cu−ZSM-5 via the reaction pathway leading to the formation of N_2O and O_2, which was experimentally observed over metal surfaces Ag(111)[34,35] and Cu(111).[36] The structure of the calculated TS with formed N−N bond (r_{N-N} = 1.18 Å) is presented in Table 5 and Figure 1 (TS). The formation of the N−N bond in the ONNO dimer is surely due to high electron donor strength of the catalytically active site and high electron

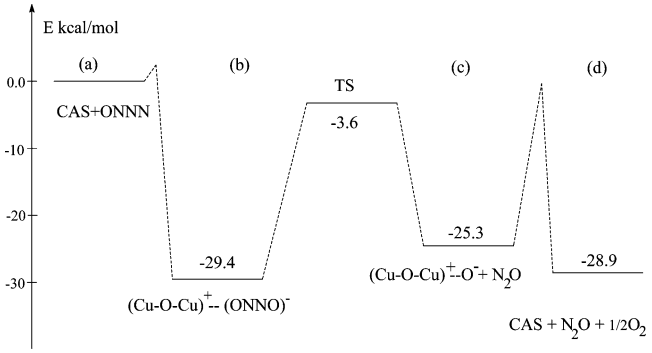

Figure 9. The energy profile of the ONNO adsorption and decomposition on the CAS in Cu−ZSM-5 zeolites: CAS(a) + ONNO ⇒ (b) ⇒ TS ⇒ $N_2O\uparrow$ + (c) ⇒ (d) (see Figure 1) calculated at the DFT/LANL2-DZ level.

affinity of ONNO, which facilitate the formation of anion π-radical structure of the transition state [q(ONNO) = −0.41, ρ_S(ONNO) = 1.21 e]. The calculated TS formation energy (ΔE = −3.7 kcal/mol) is low in comparison with the total energy of CAS and ONNO. Therefore, the ONNO decomposition activation energy must be very low. This agrees well with the experimental value of ONNO decomposition activation energy on Ag(111), which was found to be as low as 2 kcal/mol. Figure 9 presents the calculated energy profile of adsorption and sequential decomposition of the nitric oxide dimer over chain copper oxide structures (−O−Cu−O−Cu−) in the channels of Cu−ZSM-5 zeolite. The structure of the calculated (−O−Cu−O−Cu)−O_{ad} (Figure 1c) complex, which is a product of TS decomposition, is presented in Table 6. The energetic barrier between states (a) and (b) is due to intersection of adiabatic terms (^{3}A") and (^{5}A) during the formation of adsorbed ONNO anion π-radical on the catalytically active site. However, because of the energetic proximity of different spin states in CAS we estimated this barrier to equal several kcal/mol. Similarly, the barrier between states (c) and (d) related to recombination of adsorbed atomic oxygen in adjacent (−O−Cu−O−Cu)−O_{ad} chains also cannot be high because the formation of molecular oxygen is highly exothermic. All these speculations lead us to a conclusion on the possibility of low-temperature decomposition of the dimer $(NO)_2$ on copper oxide chains (−O−Cu−O−Cu−) in the channels of Cu−ZSM-5 zeolites with low activation energy.

III. Conclusions

On the basis of the B3LYP/LANL2-DZ calculations presented here, we examined (Cu−O−Cu)−ONNO complex in zeolites and discussed the formation of an N−N bond on a Cu site. DFT calculations showed that in contrast to the weakly bound cis dimer with the equilibrium distance N−N ≈ 2 Å anion radical, $(ONNO)^-$ is characterized by a strong bond between the nitrogen atoms (N−N ≈ 1.4 Å).

Analysis of the molecular orbital structure of the dimer and its anions led us to a hypothesis on the reason of preferable stabilization of the nitric oxide dimer in cis form. The calculated high electron affinity (E_a = −1.3 eV) of the ONNO dimer and significant strengthening of the N−N bond in the anion radical confirms the experimental data on the formation of surface anion π-radical on electron donor sites.

The DFT calculated electronic structure and excitation energy spectra for the model system $(HO)_3$Al−O−Cu−O−Cu show that it is a satisfactory model for description of experimental UV−vis spectra of Cu−ZSM-5, containing (−O−Cu−O−Cu−) chain structures in the zeolite channels.

The calculated reaction energy profile of ONNO adsorption and decomposition on the model catalytic active site shows the possibility of the low-temperature decomposition of dimer $(NO)_2$ with low activation energy and the important role of chain copper oxide structures (−O−Cu−O−Cu−) in the channels of Cu−ZSM-5 zeolite during selective reduction of NO.

Acknowledgment. We thank Dr. N. N. Bulgakov and Dr. G. Bogdunchikov for useful discussions. S. Ph. R. acknowledges support by the Dutch Science Foundation (in the collaborative Russian−Dutch research NWO project No. 047.015.004) and the Council of Russian President Grants (Scientific School Grant No. 1140.2003.3)

References and Notes

(1) Iwamoto, M.; Yahiro, H.; Mine, Y.; Kagawa, S. *Chem. Lett.* **1989**, 213.
(2) Iwamoto, M.; Hawada, H. *Catal. Today.* **1991**, *10*, 57.
(3) Held, W.; Konig, A.; Richter, T.; Puppe, L. *SAE Tech. Pap. Ser. 900496*, **1990**, 13.
(4) Matyshak, V. A.; Il'ichev, A. N.; Ukharsky, A. A.; Korchak, V. N. *J. Catal.* **1997**, *71*, 245.
(5) Ansell, G. P.; Diwail, A. F.; Golunski, S. E.; Hayes, J. W.; Rayaram, R. R.; Truex, T. J.; Walker, A. P. *Appl. Catal. B.* **1993**, *2*, 81.
(6) Kucherov, A. V.; Gerlock, J. L.; Jen, H.-W.; Shelef, M. *J. Catal.* **1995**, *152*, 63.
(7) Praliaud, H.; Mikhailenko, S.; Chajar, Z.; Primet, M. *Appl. Catal., B.* **1998**, *16*, 359.
(8) Cho, B. K. *J. Catal.* **1994**, *155*, 84.
(9) Petunchi, J. O.; Sill, G.; Hall, W. K. *Appl. Catal., B* **1993**, *2*, 303.
(10) Marquez-Alvarez, C.; Roriguez-Ramos, I.; Guerrero-Ruiz, A.; Fernandez-Garcia, M. The 11th International Congress on Catalysis, Baltimore, MD, June 30−July 5, 1996; p 206.
(11) Iwamoto, M.; Yahiro, H.; Murino, N.; Zhang, W.-X.; Mine, Y.; Furukawa, H.; Kagawa, S. *J. Phys. Chem.* **1992**, *96*, 9360.
(12) Valyon, J.; Hall, W. K. *J. Phys. Chem.* **1993**, *97*, 1204.
(13) Lei, G. D.; Adelman, B. J.; Sarkany, J.; Sachtler, W. M. H. *Applied Catal., B* **1995**, *5*, 245.
(14) Li, Y.; Hall, W. K. *J. Catal.* **1991**, *129*, 202.
(15) Da Costa, P.; Moden, B.; Meitzner, G. D.; Lee, D. K.; Iglesia, E. *Phys. Chem. Chem. Phys.* **2002**, *4*, 4590.
(16) Teraoka, Y.; Tai, C.; Ogawa, H.; Furukawa, H.; Kagawa, S. *Appl. Catal., A* **2000**, *200*, 167.
(17) de Carvalho, M. C. N. A.; Passos, F. B.; Schmal, M.; *Appl. Catal.* **2000**, *193*, 265.
(18) Moden, B.; Da Costa, P.; Fonfe, B.; Lee, D. K.; Iglesia, E. *J. Catal.* **2002**, *209*, 75.
(19) Groothaert, M. H.; van Bokhoven, J. A.; Battiston, A. A.; Weckhuysen, B. M.; Schoonheydt, R. A. *J. Am. Chem. Soc.* **2003**, *125*, 7629.
(20) Groothaert, M. H.; Lievens, K.; van Bokhoven, J. A.; Battiston, A. A.; Weckhuysen, B. M.; Pierloot, K.; Schoonheydt, R. A. *ChemPhysChem* **2003**, *4*, 626.
(21) Groothaert, M. H.; Lievens, K.; Leeman, H.; Weckhuysen, B. M.; Schoonheydt, R. A. *J. Catal.* **2003**, *220*, 500.
(22) Anufrienko, V. F.; Bulgakov, N. N.; Vasenin, N. T.; Yashnik, S. A.; Tsikoza, L. T.; Vosel, S. V.; Ismagilov, Z. R. *Dokl. Chem.* **2002**, *386*, 273.
(23) Anufrienko, V. F.; Yashnik, S. A.; Bulgakov, N. N.; Larina, T. V.; Vasenin, N. T.; Ismagilov, Z. R. *Dokl. Phys. Chem.* **2003**, *392*, 207.
(24) Ismagilov, Z. R.; Yashnik, S. A.; Anufrienko, V. F.; Larina, T. V.; Vasenin, N. T.; Bulgakov, N. N.; Vosel, S. V.; Tsykoza, L. T. *Appl. Surf. Sci.* **2004**, *226*, 88.
(25) Yashnik, S. A.; Ismagilov, Z. R.; Anufrienko, V. F. *Catal. Today* **2005**, *110*, 310.
(26) Yokomichi, Y.; Yamabe, T. *J. Phys. Chem.* 1**996**, *100*, 14424.
(27) Trout, B. L.; Chakraborty, A. K.; Bell, A. T. *J. Phys. Chem.* 1**996**, *100*, 17582.
(28) Ramprasad, R.; Hass, K. C.; Schneider, W. F.; Adams, J. B. *J. Phys. Chem. B* **1997**, *101*, 6903.
(29) Battiston, A. A.; Bitter, J. H.; de Groot, F. M. F.; Overweg, A. R.; Stephan, O.; van Bokhoven, J. A.; Kooyman, P. J.; van der Spek, C.; Vanko, G.; Koningsberger, D. C. *J. Catal.* **2003**, *213*, 251.
(30) Huang, Y.-J.; Wang, H. P.; Lee, J.-F. *Appl. Catal., B* **2003**, *40*, 118.

(31) Huang, Y.-J.; Wang, H. P.; Hsiao, M. C.; Tai, C. C.; Huang, H-L.; Liu, S. H. *Water, Air, Soil Pollut.* **2004**, *153*, 187.
(32) Snis, A.; Panas, I. *Chem. Phys.* **1997**, *221*, 1.
(33) Maksimov, N. G.; Dudchenko V. K.; Anufrienko, V. F.; Zakharov, V. A.; Yermakov, Yu. I. *Teor. Eksp. Khim.* **1978**, *14*, 53.
(34) Brown, W. A.; Gardner, P.; King, D. A. *J. Phys. Chem.* **1995**, *99*, 7065.
(35) Carlisle, C. I.; King, D. A. *J. Phys. Chem. B* **2001**, *105*, 3886.
(36) Dumas, P.; Suhren, M.; Chabal, Y. J.; Hirschmugl, C. J.; Williams, G. P. *Surf. Sci.* **1997**, *371*, 200.
(37) Chen, L.; Chen, H. Y.; Lin, J.; Tan, K. L. *Inorg. Chem.* **1998**, *37*, 5294.
(38) Frisch, M. J.; Trucks, G. W.; Schlegel, H. B.; Scuseria, G. E.; Robb, M. A.; Cheeseman, J. R.; Zakrzewski, V. G.; Montgomery, J. A., Jr.; Stratmann, R. E.; Burant, J. C.; Dapprich, S.; Millam, J. M.; Daniels, A. D.; Kudin, K. N.; Strain, M. C.; Farkas, O.; Tomasi, J.; Barone, V.; Cossi, M.; Cammi, R.; Mennucci, B.; Pomelli, C.; Adamo, C.; Clifford, S.; Ochterski, J.; Petersson, G. A.; Ayala, P. Y.; Cui, Q.; Morokuma, K.; Malick, D. K.; Rabuck, A. D.; Raghavachari, K.; Foresman, J. B.; Cioslowski, J.; Ortiz, J. V.; Baboul, A. G.; Stefanov, B. B.; Liu, G.; Liashenko, A.; Piskorz, P.; Komaromi, I.; Gomperts, R.; Martin, R. L.; Fox, D. J.; Keith, T.; Al-Laham, M. A.; Peng, C. Y.; Nanayakkara, A.; Challacombe, M.; Gill, P. M. W.; Johnson, B.; Chen, W.; Wong, M. W.; Andres, J. L.; Gonzalez, C.; Head-Gordon, M.; Replogle E. S.; Pople, J. A. *Gaussian 98, Revision A.11*. Gaussian, Pittsburgh, PA, 1998.
(39) Becke, A. D. *J. Chem. Phys.* **1993**, *98*, 5648.
(40) Lee, C.; Yang, W.; Parr, R. G. *Phys. Rev. B.* **1988**, *37*, 785.
(41) Hay, P. J.; Wadt, W. R. *J. Chem. Phys.* **1985**, *82*, 270.
(42) NQMLab: quantumsolutions. http://www.nqmlab.com/storage/, December 2006.
(43) Hezler, R.; Casassa, M. P.; King, D. S. *J. Phys. Chem.* **1991**, *95*, 8086.
(44) McKellar, A. R. W.; Wayson, J. K. G.; Howard, B. J. *Mol. Phys.* **1995**, *86*, 273.
(45) Kukolich, G.; Sickafoose, S. M. *Mol. Phys.* **1996**, *89*, 1659.
(46) Dkhissi, A.; Soulard, P.; Perrin, A.; Lacome, N. *J. Mol. Spectrosc.* **1997**, *183*, 12.
(47) Ochterski, J. W.; Petersson, G. A.; Montgomery, J. A. *J. Chem. Phys.* **1996**, *104*, 2598.
(48) Crutchley, R. J. *Adv. Inorg. Chem.* **1994**, *41*, 273.
(49) Parr, R. G.; Yang, W. *Density-Functional Theory of Atoms and Molecules*; Oxford University Press: New York, 1989.
(50) Runge, E.; Gross, E. K. U. *Phys. Rev. Lett.* **1984**, *52*, 997.
(51) Van Gisbergen, S. J. A.; Snijders, J. G.; Baerends, E. J. *J. Chem. Phys.* **1995**, *103*, 9347.
(52) Görling, A.; Heinze, H. H.; Ruzankin, S. Ph.; Staufer, M.; Rosch, N. *J. Chem. Phys.* **1999**, *110*, 2785.
(53) Adamo, C.; Scuseria, E.; Barone, V. *J. Chem. Phys.* **1999**, *111*, 2889.
(54) Hirata, S.; Lee, T. J.; Head-Gordon, M. *J. Chem. Phys.* **1999**, *111*, 8904.
(55) Broclawik, E.; Borowski, T. *Chem. Phys. Lett.* **2001**, *339*, 433.
(56) Ricciardi, G.; Rosa, A.; Baerends, E. J.; van Gisbergen, S. A. J. *J. Am. Chem. Soc.* **2002**, *124*, 12319.
(57) Cavillot, V.; Champagne, B. *Chem. Phys. Lett.* **2002**, *354*, 449.
(58) Frolova, Yu. V.; Avdeev, V. I.; Ruzankin, S. Ph.; Zhidomirov, G. M.; Fedotov, M. A.; Sadykov, V. A. *J. Phys. Chem. B* **2004**, *108*, 6969.
(59) Zhurko, G. A. ChemCraft. http://www.chemcraftprog.com, December 2006.
(60) Bhaduri, S.; Jonson, B. F. G.; Pickard, A.; Raithby, P. R.; Sheldrick, G. M.; Zuccaro, C. I. *J. Chem. Soc., Chem. Commun*. **1977**, 354.